doi: 10.15407/ujpe61.02.0098

V.A. ZHOVTYANSKY,[1] O.V. ANISIMOVA[2]

[1] Gas Institute, National Academy of Sciences of Ukraine
(39, Degtyarivs'ka Str., Kyiv 03113, Ukraine; e-mail: zhovt@ukr.net)
[2] National Technical University of Ukraine "Kyiv Polytechnic Institute"
(37, Peremoga Ave., Kyiv 03056, Ukraine)

ROLE OF ANODE PROCESSES IN GLOW DISCHARGE ENERGETICS

PACS 51.50.+v, 52.80.Hc

The role of anode processes in the formation of self-organized glow discharge (GD) structure is analyzed in the case of spherical diode, the latter, as well as a short plane diode, being characterized by the absence of a positive column. The results of numerical calculations are compared with the experimental GD current-voltage characteristics and the electric field strength distributions measured by the probe method. It is shown that the boundary conditions at the anode should be formulated with regard for a possibility of a potential drop at the anode. In this case, the calculated diode potential decreases significantly and corresponds to experimentally observed results.

K e y w o r d s: glow discharge, spherical diode, short diode, electric field, anode processes, fluid model, current-voltage characteristics.

1. Introduction

An important role of near-anode phenomena in the optimization of processes running in a short diode, which is a model of thermionic converter to transform thermal energy into electric one, was pointed out as long ago as in 1971 by N.D. Morgulis, the founder of the Kyiv school of physical electronics and plasma physics [1]. Really, the magnitude and the sign of a potential drop at the anode (in other words, the anode potential fall, AF) can change the final voltage at the converter and, as a result, the efficiency of its operation.

In the early scientific publications (see, e.g., work [2, sections 58 and 59]), the nature and the magnitude of AF were mainly explained on the basis of the relationship between the plasma ability to provide the anode current owing to the chaotic flow of electrons, $I_c \sim 0.25eN_e v_e S$, where e is the electron charge, N_e the electron concentration, v_e the average electron velocity, and S the area of the anode surface from the discharge side, and the discharge current I taken away from the anode into the external electric field. If $I_c > I$, there arises a negative (braking for electrons) AF, which detains some fraction of the chaotic electron flow from plasma, similarly to what an electric probe does in plasma. In the opposite case $I_c < I$, there arises a positive AF, which provides an additional generation of charged particles sufficient to compensate the difference $I - I_c$.

Experimental researches [3, 4] demonstrated that, under the glow discharge (GD) conditions, – in particular, in nitrogen – near-anode phenomena can be realized in the form of anode spots. In work [3], where the GD was generated in a tube with variable distance L between the cathode and the anode, anode spots were observed in the pressure interval $p = 0.4 \div 14$ Torr. The easiest conditions for their appearance emerged, when the distance L corresponded to the beginning of the positive column (PC) formation. On the contrary, when the anode was moved into the Faraday

dark space (FDS) region, the anode spots gradually disappeared.

Researches in work [4] were performed under conditions of a spherical GD, when the external sphere 26.7 cm in radius played the role of cathode, and the internal copper sphere 5.1 cm in diameter the role of anode. This geometry of GD was specially chosen for the optimum formation and researches of anode spots. The cited authors noted that the copper anode was always covered by a uniform discharge at every pressure $p > 1.5$ Torr and the discharge current $I_d \leq 500$ mA. If the pressure grew or the current decreased, the region of discharge contact with the anode got dimmer and acquired a diffusive character. Under the conditions of discharge in nitrogen, anode spots never appeared at $p > 1.5$ Torr, irrespective of the attained discharge current. They started to be observed at $p = 1.25$ Torr and $I = 420$ mA.

In the researches performed within recent decades (see, e.g., works [5–7]), a detailed simulation of processes in the AF region was carried out with regard for a balance between the generation and the loss of charged and neutral particles in the resonance and metastable states on the anode surface and the lateral walls of the GD tube, which confines the positive column and governs its existence.

2. Working Hypothesis

Earlier, we studied experimentally [8] and numerically [9, 10] physical processes in a spherical gas-filled diode with the aim to optimize the nitriding process (one of the surface modification methods) for metallic objects, which is executed in a nitrogen-containing atmosphere under the GD conditions (see also work [11]). Technologically, this atmosphere was created in a metallic chamber (with observation windows) of a vacuum installation, with the chamber playing the role of anode. A sample stage at the center of the chamber and objects on it, the surfaces of which were to be modified, composed a cathode. In our researches, the effective radius of the chamber (anode), $r_a \approx 20 \div 33$ cm, was much larger than the effective radius of the stage surface and objects (cathode), $r_k \approx 2$ cm [8]. This circumstance allowed the GD to be regarded as a spherical one [9]. Since $r_a \gg r_k$, the discharge was long in the geometrical sense. However, there were no transverse effects in it, which governed the structure of the GD positive column in a long cylindrical tube. The FDS in the spherical discharge is supposed to extend up to the anode (see [12] and [13, p. 547]). Really, from the physical viewpoint, there is no necessity for the PC to emerge in this case, because its role in ordinary discharges consists in the compensation of charged particle losses in the radial direction on the tube walls. It is provided by the ionization of a plasma-forming compound in the longitudinal electric field of PC to ensure the passage of the discharge current.

Visually, the GD looks like a luminous region near the cathode, with the intensity maximum being located at a distance of 2–3 cm from the latter. It includes a classical cathode layer itself and a zone of negative glow. Further, this region transforms into the FDS, which reaches the anode surface. Since, in what follows, the matter concerns the processes running near the anode, it should be noted that, under experimental conditions, no peculiarities in the radiation emission were observed visually at the FDS boundary and the chamber (anode) surface. Anode spots were not observed as well.

In this work, the numerical simulation of the processes in the AF was carried out for a spherical diode filled with nitrogen in the pressure interval $p = 0.4 \div 2$ Torr and at discharge currents $I = 10 \div 200$ mA. The cathode radius was equal to $r_k = 1.5$ cm, and the anode one to $r_a = 20$ cm. The gas temperature in the discharge was taken to be $T = 300$ K, as a rule. Calculations were carried out according to the standard hydrodynamic model of GD [14, 15]. The corresponding boundary conditions were substantiated in work [14] for a GD at $p = 5$ Torr in a short planar diode, in which the cathode and the anode are located so close to each other that the PC is absent. No ionic current was supposed to be at the anode, and the anode voltage was assumed to be known. In work [15], a similar model was used for an axially symmetric long GD between planar electrodes at the same pressure of 5 Torr, and the PC region was also taken into consideration.

Among the results of calculations obtained in works [9, 10], the attention is attracted to a considerable potential drop across some part of the discharge outside the near-cathode region. Its magnitude can amount up to half the total voltage drop across the discharge interval, depending on the GD supply regime. Formally, it looks like an extended PC region with an inherent electric field, which does not depend practi-

cally on the processes running near the cathode. However, its existence contradicts the results of experimental determination of the potential distribution along the diode radius, by using the probe method [16]: no appreciable electric field was detected there.

A working hypothesis for the explanation of this effect can be based on that the formulation of the problem in works [9, 10] supposed the existence of a substantial field outside the near-cathode region, in the gap between the electrodes. This field is required to generate charged particles in the gap, the ionic component of which should compensate a considerable bulk charge, which the electron component of the discharge current is responsible for. One may expect that the account for a possibility for the PC to be formed in the GD would "ensure" the generation of charged particles in the near-anode layer at low losses of electric power. The injection of ions from this layer into the gap between the electrodes compensates the bulk charge and eliminates the necessity for a substantial electric field to exist in the gap.

In order to specify the role of the processes running near the anode at this stage, we carried out a numerical experiment with regard for, in essence, the principle of minimum power in a gas discharge [17]. In so doing, the electric field strength at the anode $E_{\rm A}$, which can be varied, was taken as a boundary condition. The organization of this experiment became possible due to the efficiency of computations for the mathematical model of GD developed in works [9,10]. The process is based on the method of continuation of a solution in the parameter (the so-called method of quasilinearization) and allows the distributions of main discharge parameters in the whole discharge interval to be determined rather quickly in the framework of the same model [18].

3. Formulation of the Problem

The influence of anode processes on the formation of a self-organized spatial GD structure between two concentric spheres, where the internal sphere is a cathode, and the external one an anode, was studied. The researches were carried out in the framework of the hydrodynamic model, which is sufficient to illustrate the essence of the AF effect in the spherical GD.

The system consisting of equations describing the fluxes of charged particles and making allowance for the drift and diffusion flux components and the Poisson equation for the electric field strength is considered. In the spherical coordinate system in view of the symmetry of the problem, these equations look like [9, 10]:

$$\frac{1}{r^2}\frac{d}{dr}\left(r^2 J_{\rm e}\right) - \alpha(E) J_{\rm e} = 0, \tag{1a}$$

$$\frac{1}{r^2}\frac{d}{dr}\left(r^2 J_{\rm i}\right) + \alpha(E) J_{\rm e} = 0, \tag{1b}$$

$$-D_{\rm e}\frac{dN_{\rm e}}{dr} + \mu_{\rm e} N_{\rm e} E = J_{\rm e}, \tag{2a}$$

$$D_{\rm i}\frac{dN_{\rm i}}{dr} + \mu_{\rm i} N_{\rm i} E = J_{\rm i}, \tag{2b}$$

$$\frac{1}{r^2}\frac{d}{dr}\left(r^2 E\right) = \frac{e}{\varepsilon_0}\left(N_{\rm e} - N_{\rm i}\right). \tag{3}$$

Here, $J_{\rm e}$ and $J_{\rm i}$ are the absolute values of electron and ion flux densities, respectively. So that, the total discharge current equals

$$I = 4\pi r^2 e\left(J_{\rm e} + J_{\rm i}\right); \tag{4}$$

$E = -E_r$, where E_r is the radial projection of the electric field strength; $N_{\rm e}$, $D_{\rm e}$, $\mu_{\rm e}$, $N_{\rm i}$, $D_{\rm i}$, and $\mu_{\rm i}$ are the concentration, diffusion coefficient, and mobility of electrons (the subscript e) and ions (the subcript i), respectively; $\alpha(E)$ is Townsend's first ionization coefficient; e the elementary charge; and ε_0 the dielectric constant.

The boundary conditions at the cathode are:

$$J_{\rm e} = \gamma J_{\rm i}, \quad J_{\rm i} = \frac{1}{1+\gamma}\frac{j_{\rm K}}{e}, \tag{5}$$

where γ is the coefficient of secondary emission, and $j_{\rm K}$ the current density at the cathode. In accordance with our working hypothesis, the AF is positive and, hence, braking for ions. Therefore, the concentration of ions and the density of their flux at the anode are supposed to vanish:

$$N_{\rm iA} = 0, \quad J_{\rm iA} = 0. \tag{6}$$

Additionally, the value of electric field strength at the anode, $E_{\rm A}$, is supposed to be a known variable:

$$E_{\rm A} = \text{var}. \tag{7}$$

Analogously to works [9, 10], the following formula is used for Townsend's first ionization coefficient:

$$\alpha = Ap\exp\left(-\frac{Bp}{|E|}\right)\ \text{cm}^{-1}. \tag{8}$$

Here, the pressure p is reckoned in Torr units, the electric field strength E in V/cm ones, and the coefficients $A = 12$ and $B = 342$. The parameters μ_i, μ_e, D_i, and D_e in Eqs. (1) and (2) are considered to be independent of the field magnitude. Moreover, the diffusion coefficients are determined by the formulas

$$D_\mathrm{e} = \mu_\mathrm{e} k T_\mathrm{e}/e, \quad D_\mathrm{i} = \mu_\mathrm{i} k T_\mathrm{i}/e, \tag{9}$$

where k is the Boltzmann constant; the mobilities of charged particles are taken equal to $\mu_\mathrm{e} = 4.4 \times 10^5 p^{-1}$ cm^2 Torr/(V s) and $\mu_\mathrm{i} = 1.44 \times 10^3$ cm^2 Torr/(V s); the electron temperature $T_\mathrm{e} = 11600$ K, and the temperatures of ions and atoms $T_\mathrm{i} = T_\mathrm{a} = 300$ K. The coefficient of secondary ionic-electronic emission from the cathode is put equal to $\gamma = 0.1$.

4. Estimation of the Electric Field Strength at the Anode

To estimate the electric field strength at the anode, let us take advantage of the plasma electric neutrality in the main volume of GD,

$$N_\mathrm{i} = N_\mathrm{e}, \tag{10}$$

and of the circumstance that the drift components of charged particle fluxes prevail in this volume, i.e., as follows from Eqs. (2),

$$J_\mathrm{i} = \mu_\mathrm{i} N_\mathrm{i} E, \tag{11a}$$

$$J_\mathrm{e} = \mu_\mathrm{e} N_\mathrm{e} E. \tag{11b}$$

The latter factor is definitely substantiated by the results of works [9, 10] specially devoted to the study of diffusion effects in a GD. Proceeding from Eqs. (4), (10), and (11), we can determine the magnitude of ionic flux $I_\mathrm{i} = 4\pi r^2 e J_\mathrm{i}$ in the discharge interval of GD:

$$I_\mathrm{i} = \frac{\mu_\mathrm{i}}{\mu_\mathrm{e} + \mu_\mathrm{i}} I. \tag{12}$$

Just this relation has to be satisfied under the influence of AF on the basis of our working hypothesis.

Since $\mu_\mathrm{i} \ll \mu_\mathrm{e}$, a small amount of ionization events is sufficient to form I_i in the anode layer. The corresponding values of the electric field and the AF magnitude are also small. Those parameters can be determined from the following consideration [17, Ch. 14]. From Eqs. (1b) and (4), taking into account that the distance r changes relatively weakly near the anode, we obtain the formula

$$\frac{dI_\mathrm{i}}{I - I_\mathrm{i}} = -\alpha(E) dr. \tag{13}$$

In order to determine the number of ionization events, let us integrate this relation from a certain coordinate r_0 within the FDS interval near the anode (the exact position is not important, because the ionic flux practically does not change there, and Townsend's coefficient $\alpha = 0$ in the FDS interval) to the AF end:

$$\int\limits_{\frac{\mu_\mathrm{i}}{\mu_\mathrm{i}+\mu_\mathrm{e}} I}^{0} \frac{dI_\mathrm{i}}{I - I_\mathrm{i}} = -\int\limits_{r_0}^{r_\mathrm{A}} \alpha(E) dr. \tag{14}$$

In such a manner, we obtain the average number of ionization events by electrons in the AF, which is sufficient for the formed ions to maintain the plasma quasineutrality in the FDS,

$$\int\limits_{r_0}^{r_\mathrm{A}} \alpha(E) dr = -\ln\left(1 - \frac{\mu_\mathrm{i}}{\mu_\mathrm{i} + \mu_\mathrm{e}}\right) = \ln\left(\frac{\mu_\mathrm{i} + \mu_\mathrm{e}}{\mu_\mathrm{e}}\right) \approx \mu_\mathrm{i}/\mu_\mathrm{e}. \tag{15}$$

Before the changing in formula (15) from the integration over the spatial coordinate to the integration over the field, we should note that, as a result of the insignificant concentration of ions near the anode, the Poisson equation (3) in this region can be written as follows:

$$\frac{dE}{dr} = \frac{e}{\varepsilon_0} N_\mathrm{e}. \tag{16}$$

Using now this relation in Eq. (15), we obtain the equation for the field strength,

$$\int\limits_{0}^{E_\mathrm{A}} \frac{\alpha(E) dE}{\frac{e}{\varepsilon_0} N_\mathrm{e}} = \frac{\mu_\mathrm{i}}{\mu_\mathrm{e}}. \tag{17}$$

The lower limit of integration can be put equal to zero, because the charge generation is practically absent ($\alpha = 0$) at the field values lower than those in the FDS, $E \approx 2 \div 5$ V/cm.

In order to obtain a simple estimate "from above" for the electric field at the anode, let us use the fact that dependence (8) for $\alpha(E)$ has a sharp exponential

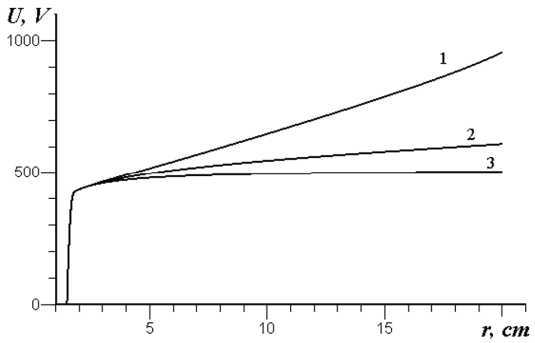

Fig. 1. Distributions of the potential U in the interelectrode interval of a spherical GD: without the AF (*1*) and taking the AF into account at the field strength at the anode $E_{\rm A}^{*}$ (*2*) and $E_{\rm Af}$ (*3*). The discharge current $I = 100$ mA, and the pressure $p = 150$ Pa

character. Let us determine such a field magnitude $E_{\rm Af}$ that would be sufficient not only for condition (17) to be satisfied, but additionally create a diffusion electron flux $J_{\rm e\,dif}$ directed to the cathode (in the opposite direction to the drift component of flux $J_{\rm e\,dr}$) and strongly exceeding $J_{\rm e}$. In this case, a simple final expression can be obtained, because the relation $J_{\rm e\,dr} \approx J_{\rm e\,dif} \gg J_{\rm e}$ is obeyed, and, accordingly, we may set the diffusion and drift fluxes equal to each other,

$$D_{\rm e}\frac{dN_{\rm e}}{dr} = \mu_{\rm e}N_{\rm e}E. \tag{18}$$

Now, we should substitute the value of $N_{\rm e}$ from Eq. (16) into this formula and integrate the result along the AF interval,

$$D_{\rm e}\int\limits_{N_{\rm e0}}^{N}\frac{dN_{\rm e}}{dr} = \mu_{\rm e}\frac{\varepsilon_0}{e}\int\limits_{0}^{E}E\frac{dE}{dr}.$$

As a result, we determine a relation between the field strength and the electron concentration near the anode,

$$N_{\rm e} = N_{\rm e0} + \frac{\varepsilon_0}{e}\frac{\mu_{\rm e}}{2D_{\rm e}}E^2, \tag{19}$$

where $N_{\rm e0}$ is a quantity, whose order of magnitude corresponds to the electron concentration in the FDS interval.

Substituting expression (8) for the first ionization coefficient and expression (19) for the electron concentration (without the neglected term $N_{\rm e0}$) into Eq. (17), we obtain the sought value of electric field strength at the anode. Really,

$$\int\limits_{0}^{E_{\rm Af}}\alpha(E(r))dr = \int\limits_{0}^{E_{\rm Af}}\frac{2D_{\rm e}A}{\mu_{\rm i}B}\exp\left(-\frac{B_p}{|E|}\right)d\left(-\frac{B_p}{E}\right) =$$
$$= \frac{2D_{\rm e}A}{\mu_{\rm i}B}\exp\left(-\frac{B_p}{E_{\rm A}}\right) = \frac{\mu_{\rm i}}{\mu_{\rm e}},$$

whence

$$E_{\rm Af} = \frac{B}{\ln\left(\frac{2D_{\rm e}A}{\mu_{\rm i}B}\right)}p. \tag{20}$$

In Fig. 1, the examples of calculated potential distributions in spherical GDs are shown. First of all, the attention is attracted to that the result determined in accordance with works [9, 10] and corresponding to the boundary condition at the anode $dN_{\rm e}/dr = 0$ (curve *1*) testifies to a considerable potential growth $\Delta U \approx 500$ V outside the cathode layer, which can attain half the total voltage drop across the discharge interval. Just this fact makes this region formally similar by its properties to the "positive column", in which ions compensating the bulk charge are generated. However, the existence of such a region contradicts the results of probe measurements of the spatial potential distribution [16, 19].

At the same time, if, in accordance with Eq. (20), the field at the anode is put equal to $E_{\rm Af}$, a substantial reduction of the voltage drop across the FDS interval to a level $\Delta U \approx 50$ V is obtained (curve *3*), which is an order of magnitude smaller than that calculated taking no AF into account. The formation of ions in this case is localized to the AF interval.

5. Specification of Processes Running in the AF Interval

In order to further optimize the operating mode of the diode, the dependence of the voltage difference across the discharge interval, U_d, on the field at the anode, $E_{\rm A}$, is researched. Its typical example is shown in Fig. 2. As $E_{\rm A}$ grows, the value of U_d changes weakly at first. When $E_{\rm A}$ achieves a certain critical value, the electrode voltage drastically decreases. A further increase of $E_{\rm A}$ is accompanied by a small reduction of the voltage, but the resulting curve has no minimum. Mathematically, the inflection point in the dependence $U_d(E_{\rm A})$, where the magnitude of the curve

slope is maximum, was selected as a characteristic value $E_{\rm A}^*$ of the electric field at the anode in the AF. Figure 1 illustrates the dependence of the potential distribution on the spatial coordinate in the diode at the selected value of the field at the anode (curve *2*), which is an intermediate one with respect to the previous data.

The characteristic value $E_{\rm A}^*$ of the field at the anode almost does not depend on the discharge current I. For instance, at the pressure $p = 150$ Pa and the current varied from 20 to 200 mA, it weakly changes within an interval of 113.6–115.3 V/cm. A certain growth of $E_{\rm A}^*$ with the current can be explained by the growth of carrier concentration in the FDS (as a result, the neglected quantity $N_{\rm e0}$ in Eq. (19) increases).

The value of $E_{\rm A}^*$ almost linearly depends on the pressure p (Fig. 3). This behavior corresponds to relation (20), according to which the upper estimate for the characteristic field strength at the anode $E_{\rm Af}$ is also proportional to the pressure and does not depend on the discharge current I. Expectedly, $E_{\rm A}^* < E_{\rm Af}$, but the difference between them is insignificant. For example, $E_{\rm A}^* = 114.6$ V/cm and $E_{\rm Af} = 126.4$ V/cm at the pressure $p = 150$ Pa and the discharge current $I = 100$ mA.

In Figs. 4 and 5, the radial distributions of the field E and the electron, $N_{\rm e}$, and ion, $N_{\rm i}$, concentrations in the spherical diode are shown for various boundary conditions at the anode. Those plots visually demonstrate a correlation between the effects associated with the generation of ions in the AF interval under the influence of a local electric field. When the field at the anode achieves the value of $E_{\rm A}^*$, the concentration of charges considerably increases (Fig. 5, curve *2*), and the field in the FDS decreases by an order of magnitude (Fig. 4, curve *2*), so that a positive potential jump that is formed in the AF interval has a magnitude of about several volts. The thickness of the AF localization region where the basic potential drop takes place amounts to $\delta_{\rm A} = 0.02$ cm at a pressure of 150 Pa. Near the anode, the distributions of the field, $E(r)$, and concentrations, $N_{\rm e}(r)$ and $N_{\rm i}(r)$, are almost identical for various values of discharge current I.

As is shown in Fig. 6, the ionic current $I_{\rm i}$ is generated in the AF in a thin layer adjacent to the anode (curves *2* and *3*). In the FDS region, the ionic current remains constant, and its fraction $I_{\rm i}/I$ is

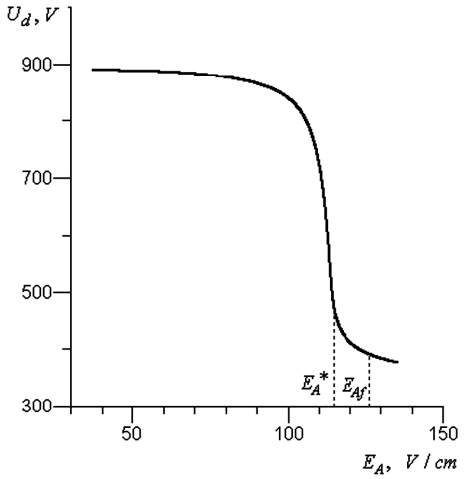

Fig. 2. Dependence of the voltage U_d between the GD electrodes on the field strength at the anode $E_{\rm A}$. The discharge current $I = 100$ mA, and the pressure $p = 150$ Pa

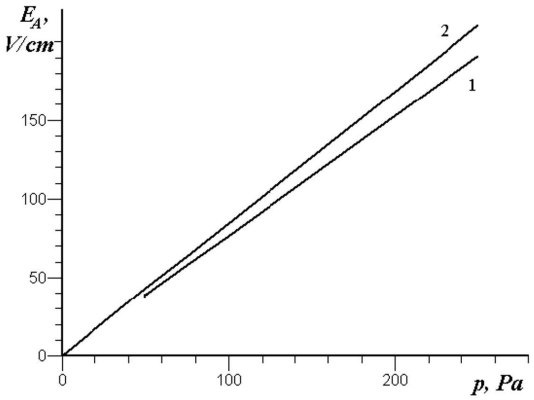

Fig. 3. Pressure dependences of the characteristic fields at the anode in the AF: $E_{\rm A}^*$ (*1*, the discharge current $I = 100$ mA) and $E_{\rm Af}$ (*2*)

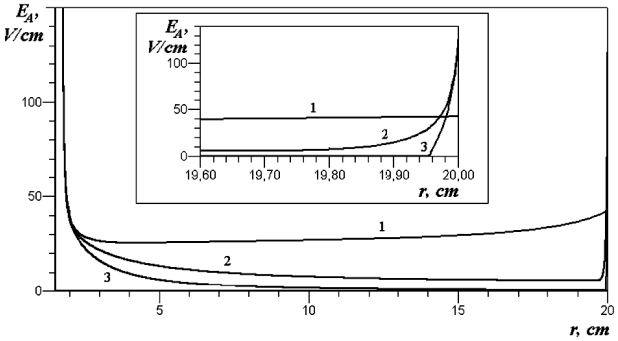

Fig. 4. The same as in Fig. 1, but for the field strength $E_{\rm A}$

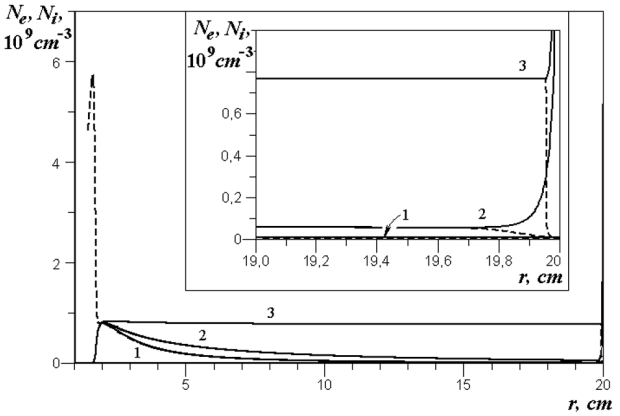

Fig. 5. The same as in Fig. 1, but for the electron (N_e, solid curves) and ion (N_i, dashed curves) concentrations

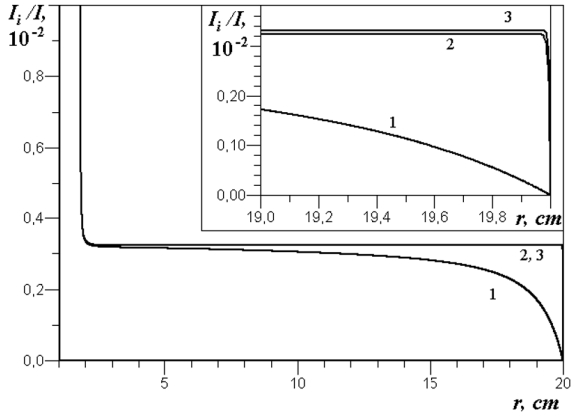

Fig. 6. The same as in Fig. 1, but for the ionic current fraction I_i/I

close to $\mu_\mathrm{i}/\mu_\mathrm{e}$. In the case $E_\mathrm{A} = E_\mathrm{A}^*$ (curve *2*), $I_\mathrm{i}/I = 3.25 \times 10^{-3}$, which is almost equal to $\mu_\mathrm{i}/\mu_\mathrm{e} = 3.3 \times 10^{-3}$. In the absence of AF, the generation would take place directly in the FDS, which would correspond to rather a high value of the field in this region (about 20 V/cm).

As the field at the anode increases, $E_\mathrm{Af} > E_\mathrm{A}^*$, the ionic current fraction grows (it can exceed $\mu_\mathrm{i}/\mu_\mathrm{e}$), the ionic current in the FDS remains constant, the field in the FDS decreases, the concentrations of electrons at the anode and charges in the FDS grow, the field strength profile approaches a linear one, and the anode layer becomes a little thinner (curve *3*).

It should be noted that, under the conditions that are characteristic of Figs. 1 to 6 (a pressure of 150 Pa and a temperature of 300 K), the mean free path of electrons $\lambda_\mathrm{e} = (\sigma N_g)^{-1}$, where σ is the collision cross-section and $N_g = 3.62 \times 10^{16}$ cm^{-3} is the concentration of atoms in the gas, amounts to $\lambda_\mathrm{e} = 0.0084$ for $\sigma = 3.3 \times 10^{-15}$ cm^2 [20] According to the most careful estimates [21], $\sigma = 2.1 \times 10^{-15}$ cm^2 for 2.8-eV electrons, so that $\lambda_\mathrm{e} = 0.013$. Nevertheless, $\delta_\mathrm{A} \geq \lambda_\mathrm{e}$ in both cases.

In the case $E_\mathrm{A} = E_\mathrm{Af}$ (curve *3*), the ionic current fraction I_i/I in the FDS can be both larger (at low currents) and smaller (at large currents) than $\mu_\mathrm{i}/\mu_\mathrm{e}$. However, those deviations are insignificant. The reduction of I_i/I, as the current grows, can be explained by an increase of the charge carrier concentration in the FDS (the neglected N_e0 grows). The fact that $I_\mathrm{i}/I > \mu_\mathrm{i}/\mu_\mathrm{e}$ for small currents can be explained by the influence of ions in the anode region. Really, the concentration of ions was not taken into account as the term $-N_\mathrm{i}$ on the right-hand side of formula (16). Therefore, when determining the field strength gradient according to expression (17), the denominator has to decrease at the transition from the anode to the FDS region. Accordingly, the integral (the number of ionization events) will grow, which will give rise to the growth of the ionic current.

6. Influence of AF on the Energetics of Processes in GD

As follows from the consideration above, the adequacy of taking the role of anode processes into account can be a very important factor when designing the equipment, in which the GD is used, and, in particular, when substantiating such operation conditions for this equipment that would be the most effective energetically. As an example, let us consider an application of the proposed approach to a real installation for nitriding the surface of metallic objects in GD plasma [8, 22]. In this case, discharge plasma was formed in nitrogen (or an N_2–Ar mixture) at a pressure of 50–250 Pa and the discharge current $I \leq 120$ mA. Specimens to be nitrided were mounted on a metallic sample stage 5 cm in diameter (together, they played the role of cathode) in the central part of the vacuum chamber (the anode). Nitriding was carried out after the chamber evacuation and a preliminary treatment (cleaning) of the specimen surface in the GD in the pure argon atmosphere. Nitriding itself was carried out in nitrogen or in its mixture with argon. The temperature of the stage plate and the specimens during this process was maintained in the interval from 810 to 820 K, which was optimal for

the process to be efficient. The objects were heated by the GD, and, for this reason, the GD power was maintained at the constant level $U_d I \approx 60$ W during the nitriding process. The cathode temperature was monitored with the help of a thermocouple.

The DC supply voltage U across the GD was varied up to 1500 V, and the corresponding current-voltage characteristics (CVCs) of this discharge were measured. At each measurement, the equilibrium temperature of the cathode with respect to its Joule heating and thermal and radiation losses was attained.

At the numerical simulation, this system was approximated as a spherical diode with the cathode radius $r_k = 1.5$ cm and the anode radius $r_a = 33$ cm; the validity of this approximation was shown in work [9]. In some cases, experimental researches were also carried out with a spherical molybdenum cathode.

The set of solutions for the system of equations (1)–(4) allows one to determine the CVC of the discharge in this diode with those or other boundary conditions theoretically and compare them with experimental data. First, CVCs in the case of the standard boundary conditions (5) and (6) with the additional condition $dN_e/dr = 0$ at the anode were determined. As follows from Fig. 7, *a*, their comparison with experimental data testifies to a very weak correlation between two CVC groups.

Bearing in mind that neglecting the radial nonuniformity of the gas temperature in the diode owing to a high cathode temperature could be responsible for this discrepancy, the system of equations (1)–(4) was appended with the thermal conductivity equation

$$\frac{1}{r^2}\frac{d}{dr}\left(r^2\kappa\frac{dT}{dr}\right) = 0, \tag{21}$$

where

$$\kappa = \frac{8.334\times10^{-4}}{\sigma^2\Omega^{(2,2)}}\sqrt{\frac{T}{M}}\left(0.115 + 0.354\frac{c_p M}{R}\right) \tag{22}$$

is the thermal conductivity coefficient [15], M the molar mass, $\Omega^{(2,2)} = 1.157(71.4/t)^{0.1472}$, $\sigma = 3.68$ Å, and $R = 8314$ J/(mol K). Taking this effect into account, the gas temperature in the discharge interval changes from 800 K at the cathode to 400 K at a distance of 5 cm from it. However, the account of this temperature nonuniformity did not improve the correspondence between the calculated and experimentally measured (Fig. 7, *b*, curve *10*) CVCs.

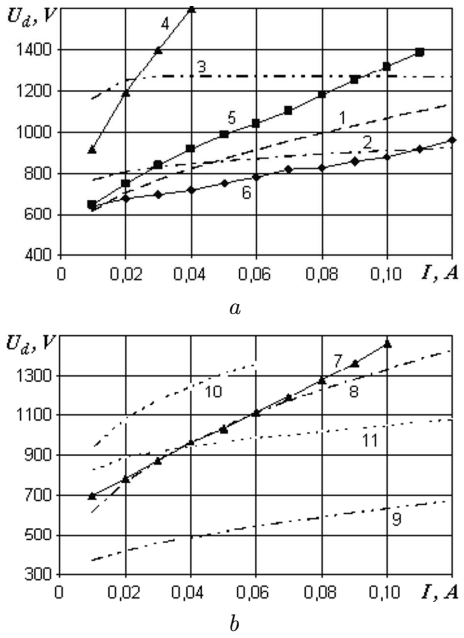

Fig. 7. Experimental (solid curves) and numerically calculated (dashed curves) CVCs of a spherical GD ($r_k = 1.5$ cm) in the absence of AF at pressures $p = 50$ (*1, 4*), 120 (*2, 5*), and 250 Pa (*3, 6*) (*a*); at a pressure of 100 Pa: experiment (*7*) and numerical simulation data taking the AF into account at $T_K = 800$ (*8*) and 300 K (9), and in the absence of AF at $T_K = 800$ (*10*) and 300 K (*11* (*b*))

The account of the influence of AF on the GD parameters became a key factor in this aspect. The system of equations (1)–(4) and (21) was solved with boundary conditions (5)–(7), when the electric field strength at the anode was put equal to E_A in accordance with Eq. (20). As one can see from the comparison of curves *7* and *8* in Fig. 7, *b*, the CVC of a GD in the course of nitriding can be described rather adequately in this case. A further improvement can be reach by the additional consideration of a variation of the instant cathode temperature in accordance with changing the power, as the voltage across the discharge interval increases or decreases.

7. Conclusions

To summarize, it is shown in this work that the compensation of the bulk charge in the interval between the electrodes is an important function of the anode processes in a GD. This function manifests itself especially brightly in a short diode, where there are no alternative mechanisms of such a compensation asso-

ciated with ionization processes in the PC. By their physical properties, the spherical diodes are classed to short diodes, irrespective of the ratio between their cathode and anode radii. Really, no necessity in the PC appearance arises in this case, because its role in ordinary discharges consists in the compensation of losses by charged particles in the radial direction at the tube walls, which is provided by the ionization of the plasma-forming compound in the longitudinal electric field of a PC to provide the passage of the GD current.

Main regularities of the AF region formation in the spherical diode are determined. The account of this region is shown to result in a considerable reduction of the calculated potential drop at the GD electrodes. A physical reason for this effect consists in the generation of charged particles in the AF at a low electric power consumption, the ionic component of which provides the compensation of the bulk charge in the FDS interval. An issue concerning the absence of a minimum in the functional dependence of the potential drop at the GD electrodes, U_d, on the electric field at the anode in the AF interval near $E_{\rm A}$ remains open to discussion. A probable reason consists in that, in the framework of the hydrodynamic model, electrons "do not know" that their capabilities to use the potential at collisions are restricted, because the effective AF thickness is comparable with the characteristic mean free path of electrons, $\delta_{\rm A} \sim \lambda_{\rm e}$, and continues to decrease as $E_{\rm A}$ grows.

The adequate account of the AF role makes it possible to optimize the GD simulation from the viewpoint of the GD application to a plasma-assisted modification of the surface of metallic objects, bearing in mind to achieve the best power efficiency.

This work was supported by the National Academy of Sciences of Ukraine in the framework of the program "Prospective study of plasma physics, controlled thermonuclear fusion, and plasma technologies".

1. N.D. Morgulis, A.I. Kravchenko, and V.Ya Chernyak, Zh. Tekhn. Fiz. **27**, 2385 (1972).
2. V.L. Granovskii, *Electric Current in Gas. Steady-State Current* (Nauka, Moscow, 1971) (in Russian).
3. C.H. Thomas and O.S. Duffendack, Phys. Rev. **35**, 72 (1930).
4. S.M. Rubens and J.E. Henderson, Phys. Rev. **58**, 446 (1940).
5. Yu.B. Golubovskii, V.I. Kolobov, and Sh.Kh. Al-Shavat, Zh. Tekhn. Fiz. **58**, 1729 (1988).
6. C. Wilke, H. Deutsch, A. Dinklage, and H. Scheibner, Czech. J. Phys. **48**, 1167 (1998).
7. S. Arndt, F. Sigeneger, and R. Winkler, Plasma Chem. Plasma Process. **23**, 439 (2003).
8. O.G Didyk, V.A. Zhovtyansky, V.G. Nazarenko, and V.A. Khomych, Ukr. Fiz. Zh. **53**, 481 (2008).
9. V.A. Zhovtyansky and Yu.I. Lelyukh, Ukr. Fiz. Zh. **53**, 495 (2008).
10. V.A. Zhovtyansky and Yu.I. Lelyukh, Pis'ma Zh. Tekhn. Fiz. **35**, 81 (2009).
11. V.A. Zhovtyansky and A.V. Anisimova, Ukr. Fiz. Zh. **59**, 1155 (2014).
12. L.B. Loeb, *Fundamental Processes of Electrical Discharge in Gases* (Wiley, New York, 1955).
13. A.A. Kudryavtsev, A.S. Smirnov, and L.D. Tsendin, *Physics of Glow Discharge* (Lan', St.Petersburg, 2010) (in Russian).
14. Yu P. Raizer and S.T. Surzhikov, Teplofiz. Vys. Temp. **28**, 439 (1990).
15. A.S. Petrusev, S.T. Surzhikov, and J.S. Sheng, Teplofiz. Vys. Temp. **44**, 814 (2006).
16. V. Zhovtyansky, V. Khomych, Yu. Lelyukh *et al.*, in *Proceedings of the 6-th International Conference on Plasma Physics and Plasma Technology* (Minsk, Belarus, 2009), Vol. 1, p. 163.
17. Yu.P. Raizer, *Gas Discharge Physics* (Springer, Berlin, 1997).
18. Yu.I. Lelyukh, Ukr. Fiz. Zh. **55**, 1165 (2010).
19. V.A. Khomich, A.V. Ryabtsev, E.G.Didyk *et al.*, Pis'ma Zh. Tekhn. Fiz. **36**, 91 (2010).
20. A.V. Yeletskii, L.A. Palkina, and B.M. Smirnov, *Transfer Phenomena in Weakly Ionized Plasma* (Atomizdat, Moscow, 1975) (in Russian).
21. A.V. Phelps, J. Phys. Chem. Ref. Data **20**, 557 (1991).
22. V.A. Zhovtyansky, O.V. Anisimova, V.O. Khomych *et al.*, Probl. At. Sci. Technol. No. 1, 95 (2011).

Received 08.02.15.
Translated from Ukrainian by O.I. Voitenko

В.А. Жовтянський, *О.В. Анісімова*

РОЛЬ ПРИАНОДНИХ ПРОЦЕСІВ
В ЕНЕРГЕТИЦІ ЖЕВРІЮЧОГО РОЗРЯДУ

Р е з ю м е

Проаналізовано роль прианодних процесів у формуванні самоорганізованої структури жевріючого розряду (ЖР) на прикладі сферичного діода. Його особливість, як і короткого плоского діода – відсутність позитивного стовпа. Дослідження виконане методом чисельного експерименту, результати якого порівнюються з вимірюваннями вольт-амперних характеристик ЖР та напруженості електричного поля зондовим методом. Показано, що граничні умови на аноді повинні формулюватися з урахуванням можливості формування прианодного скачка потенціалу. Це значно зменшує розрахункове падіння потенціалу на діоді, що відповідає експериментальним результатам.